PCCP

Accepted Manuscript

ROYAL SOCIETY OF CHEMISTRY

www.rsc.org/pccp

Journal Name

RSCPublishing

ARTICLE

Giant Conductivity Enhancement of Ferrite Insulators Induced by Atomic Hydrogen

Cite this: DOI: 10.1039/xoxxoooooox

Qing-Yun Xiang,[a] Yu Wang,[b] Shi-Yu Li,[a] Lan-Hua Wang,[a] Li-Bin Mo,[a] Wen-Qing Yao,[c] Li Zhang[d] and Jiang-Li Cao[a, d*]

Received ooth January 2012,
Accepted ooth January 2012

DOI: 10.1039/xoxxoooooox

www.rsc.org/

Hydrogen behaviors in oxides have triggered much interest for their scientific and technological importance in a wide range of research fields from novel ion conductors to astrochemistry. Here, we report a giant conductivity enhancement in $ZnFe_2O_4$ ferrite insulators to metallic state by over eleven orders of magnitude induced by electrochemically-generated atomic hydrogen at room temperature. Quantitative kinetics correlations among the adsorption of atomic hydrogen, hydrogen incorporation and conductivity enhancement are established, based on which a hydrogen incorporation process is clarified herein. We demonstrate that the hydrogen incorporation in oxides can be adjusted by manipulating the kinetic factors. These findings give implications for research of hydrogen behaviors in oxides in hydrogen atoms-containing environments and offer possibilities for utilizing and controlling modifications of oxide materials induced by atomic hydrogen.

1. Introduction

In recent years, behaviors of hydrogen and its isotopes in oxide materials started to attract rapidly increasing attention.[1,2] These oxides are of inestimable importance and distinguish themselves in many scientific and technological fields such as thermonuclear fusion reactors,[3,4] astrochemistry,[5] hydrogen production and storage,[6-9] fuel cells,[10,11] information technologies,[12] etc. Although specific research emphases vary from areas to areas, the common ground of hydrogen-related oxides lies in that these materials are exposed to elementary hydrogen-containing environments during formation processes or under working conditions,[13,14] i.e. molecular, atomic and ionized hydrogen. Atomic hydrogen is present widely, e.g. under electrochemical cathodic or photochemical conditions, in metals and outer space, etc. The underlying fundamental issues are worthwhile to study because of the generality and importance of hydrogen behaviors in oxides. As one of these focal points, hydrogen-induced modifications are common for various oxide materials and to a wide range of properties such as electrical, optical and magnetic properties.[15-18]

Atomic hydrogen-induced modifications in oxide materials have been reported in the last decade, for example, researches about TiO_2,[19,20] ZnO,[21] Nb_2O_5,[22] NiZnCu-based ferrite,[23] $Pb(Mg,Nb)O_3$[24] and $Pb(Zr,Ti)O_3$,[25] showed changes in electrical properties and were generally ascribed qualitatively to the generation of electronic carriers and oxygen vacancies due to reduction of metal ions by hydrogen. Naturally, the modifications in a wider range of oxides with greater diversities are expectable. Nevertheless, the general physical correlation between the modifications and hydrogen penetration is yet missing. The kinetics of the atomic hydrogen penetration and modifications in oxide materials has hardly been investigated, however, which is indispensable to understanding the hydrogen behaviors and to further utilizing and controlling these behaviors.

Ferrites are widely used to manufacture electromagnetic wave absorbing materials, transformers, catalysts and so on in the areas of military industries, information technologies and energy technologies owing to their useful and diversified properties.[26-28] As well known, iron is the fourth and fifth most abundant element in the earth crust and on the moon,

respectively, making iron-based oxides of great scientific and technological interest. Because of the important role of iron-based oxides in modern scientific and application areas, a deep insight into the hydrogen behaviours may lead to significant progress in relevant fields. Here, we report the induced giant conductivity enhancement and the atomic hydrogen incorporation behaviors in a model oxide material, i.e. $ZnFe_2O_4$ ferrite.

2. Experimental Section

The spinel ferrite $ZnFe_2O_4$ was prepared through the following steps. First, ceramic powders were synthesized through a solid-state reaction method and ball-milled in ethanol for 24 hours with polyvinyl alcohol as binder. The obtained pastes were degassed under slow stirring for 24 hours followed by tape casting into green sheets. Second, pellets of 1.2 mm thick were obtained by punching the green sheets and then sintered at 1150 °C for 2 hours. Finally, spinel ferrite samples of 10 mm in diameter were prepared and silver electrodes were fired onto both sides of the pellets for electrical measurements.

The atomic hydrogen charging was carried out under cathodic electrochemical conditions through electrolysis with vibration (Supplemental Fig. 1). The electrolyte was 0.1 mol/l Na_2SO_4 water solution with a pH value of 7. Chelating agent Na_2EDTA was added in the solution as absorbate to modify the atomic hydrogen adsorption. The cathodic current density was kept constant at 38 A/m^2. Conductive copper balls of 2 mm in diameter were used as the cathode. After the electrochemical hydrogen charging, the ferrite samples were cleaned using deionized water and then dehydrated.

The apparent direct current conductivity was measured at room temperature using an HP4140B pA meter and Fluke 8846A multimeter. Microstructures of the samples were examined using field emission scanning electron microscopy (SEM, ZEISS Supra-5). The amount of incorporated hydrogen in ferrites was measured by a diffusible hydrogen analyzer (DHA, BRUKER G4-Phoenix) using a thermal conductivity detector by heating samples to 820 °C in pure N_2.

The surface layer of ferrite pellets was removed using diamond blades and collected for X-ray diffraction measurement (XRD, Bruker D8 Advance Diffractometer) at room temperature with Cu Kα radiation.

X-ray photoelectron spectroscopy (XPS) analyses were conducted to examine the chemical environments of compositional elements on the ferrite surface using a PHI Quantera SXMX with a spherical capacitance analyzer. Al Kα x-rays were adopted as the excitation source operating at 26.5 W with a take-off angle of 45°; electron binding energies were calibrated against the reference peak of C 1s (284.8 eV).

3. Results and Discussion

3.1 Atomic hydrogen-induced modifications.

The insulating ferrite surface became conductive upon atomic hydrogen charging and turned from blue to black. Figure 1 plots the apparent conductivity σ of the ferrite as a function of the atomic hydrogen charging time. The virgin insulating ferrite had a low conductivity of 2.40×10^{-10} S/m. The conductivity increased drastically within ten minutes of atomic hydrogen charging. Then the conductivity continues to increase more slowly with increasing hydrogen charging time and has an enhancement of over eleven orders of magnitude at last. It is naturally expected that hydrogen may have incorporated into the ferrite surface. Therefore, we measured the amount of incorporated hydrogen q in the ferrite of the whole sample using DHA as a function of the charging time t (Fig. 1). The diffusible hydrogen amount increased with charging time and reached as high as 14 ppm in 40 minutes.

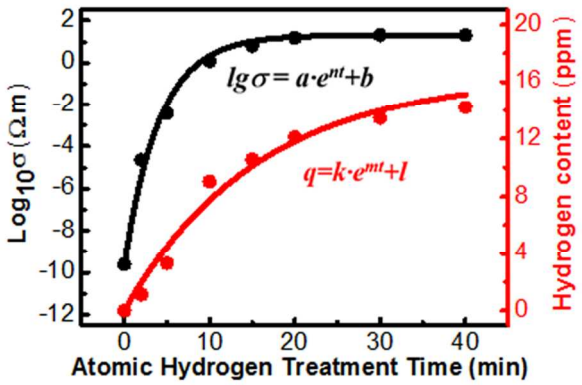

FIGURE 1. The atomic hydrogen-induced conductivity enhancement of ferrite insulators and the content of incorporated hydrogen expressed as parts per million (ppm) by weight. The experimental data are given in solid circles. Best fits to the experimental data using a least-squares method are shown in line and the goodness of fit R is 0.9912 and 0.9774, respectively.

SEM observations and XPS surface analyses were conducted with an as-sintered and a 40 min H-charging ferrite samples. The as-sintered ferrite is dense and has a granular structure (Fig. 2a). By contrast, some cracks appeared on the surface of the H-charged sample (Fig. 2b). The Fe 2p3/2 peak of the as-sintered sample in Fig. 2a is symmetrical and contains only one Gaussian component. The Fe 2p3/2 binding energy measures 711.8 eV, indicating that iron ions are all in the +3 state. However, the shape of the Fe 2p3/2 peak of the charged sample changes remarkably (Fig. 2b). Through best fit, the Fe 2p3/2 peak is decomposed into two Gaussian components with a binding energy of 711.9 eV and 710.5 eV, corresponding to Fe^{3+} and Fe^{2+}, respectively.[29] The Fe^{3+}: Fe^{2+} mole ratio at the surface is calculated to be 66:34. No evident chemical shifts were observed for the Zn at A-site in the present study.

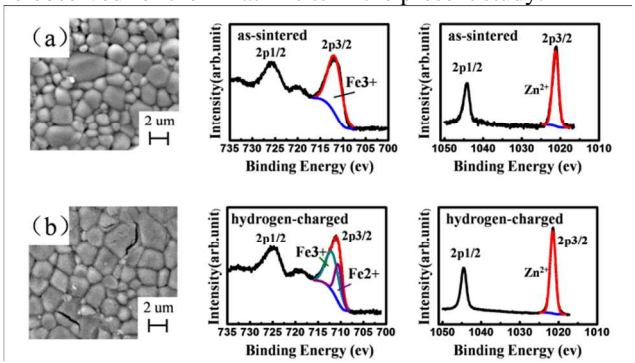

FIGURE 2. SEM micrographs and XPS spectra of the $ZnFe_2O_4$ spinel ferrites (a) before and (b) after the 40 min electrochemical atomic hydrogen charging.

Therefore, the giant conductivity enhancement of the ferrite insulators is tentatively ascribed to the formation of a donor energy level due to reduction of Fe^{3+} to Fe^{2+} induced by the incorporated hydrogen. XRD analyses revealed that most of the specimens remained the spinel phase structure, and a rightward shift of diffraction peaks was found after the hydrogen incorporation, which suggests a decrease of the lattice spacing. Meanwhile, the crystallinity became worse and a new peak was formed around 44.3° upon hydrogen charging (Supplemental Fig. 2). The 44.3° peak is tentatively ascribed to the iron hydride according to JCPDS file 43-1321.[30] Future detailed studies will be conducted for clarifying the fine structure of this hydrogenated ferrite.

3.2 The hydrogen incorporation model.

The conductivity enhancement could be correlated with the hydrogen incorporation process during atomic hydrogen charging and explained in the following steps according to adsorption theory and electrochemistry. First, hydrated hydrogen ions receive an electron on the cathode surfaces in the electrolyte under the cathodic current and highly active hydrogen atoms are generated (step 1 of Fig. 3).[15,19] Most of these hydrogen atoms recombine into chemically stable hydrogen molecules through Volmer-Tafel or Volmer-Heyrovsky desorption,[31] enter into the electrolyte directly through desorption while some remaining hydrogen atoms could replace the adsorbing water molecules when moving to the oxide surfaces and be adsorbed (see step 2 in Fig. 3).[32] Covalent forces would involve through electrons sharing between the adsorbent and adsorbate according to the adsorption theory. With increasing charging time, the coverage of atomic hydrogen will increase until saturation, which corresponds to an equilibrium state. Second, the adsorbed hydrogen atoms are dissolved into the lattice of the outmost surface of the ferrites (see step 4 in Fig. 3). The chemical structure of the oxides would be altered once hydrogen atoms are incorporated into the oxide lattice. Consequently, the dissolved hydrogen atoms result in the reduction of Fe^{3+} to Fe^{2+} in the ferrites, as observed by XPS analyses in this study. Third, the dissolved hydrogen diffuse toward the bulk of the oxides under chemical potential caused by the concentration gradient (see step 5 in Fig. 3). Through examinations of the cross section, the diffusion characteristics of hydrogen could be evaluated, as reported earlier.[24,25] It is known that hydrogen diffusion in oxides at low temperatures is normally slow.[32] Therefore, the diffusion step is slower than the adsorption and dissolution generally. With more adsorbed hydrogen atoms being dissolved, the oxide surfaces become more conductive and the measured conductivity increases remarkably in the initial 10 minutes. According to Sieverts' law, the concentration of dissolved hydrogen could increase until its saturation solubility. Therefore, the approaching of either the hydrogen adsorption coverage or concentration of dissolved hydrogen in the surface lattice to a saturation state may result in a decrease of the conductivity enhancement rate with increasing hydrogen charging time. Eventually, the conductivity and the hydrogen content of ferrites tend to reach stable, as observed in Fig. 1.

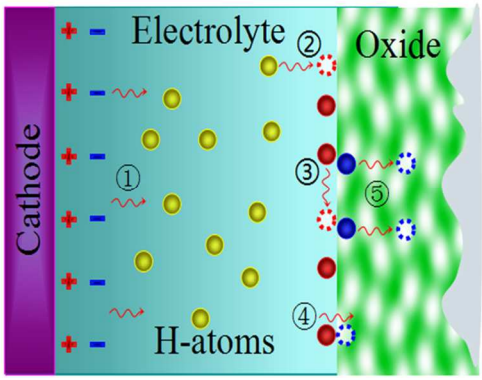

FIGURE 3. Incorporation of atomic hydrogen into oxide materials from the electrolyte under electrochemical conditions. ① Generation of hydrogen on the cathode. ② Hydrogen adsorption. ③ Diffusion of adsorbed hydrogen atoms. ④ Dissolution of adsorbed hydrogen into the oxide. ⑤ Hydrogen diffusion in the oxide under chemical potential. The dashed circles indicate the hydrogen migration to a next position.

3.3 Kinetics relationship.

Atomic hydrogen charging experiments using Na_2EDTA as additive were conducted to further clarify the correlation between the hydrogen incorporation and material modifications. The chelating agent Na_2EDTA is a well-known adsorbate and can form complexes with many species of metal ions.[33,34] The hydrogen incorporation process proposed above is well supported by the experimental findings, which can be interpreted according to the chemisorption theory. Na_2EDTA exhibits well-defined effects on the conductivity transformation of the ferrite insulators and the hydrogen incorporation, in accordance with the kinetics equations. With increasing Na_2EDTA concentration, the conductivity transformation and hydrogen incorporation occur much more slowly and the extents become evidently smaller (Fig. 4(a)). XRD result of 40 min hydrogenated samples with Na_2EDTA as additive was performed (Supplemental Fig. 2). The main structure maintained spinel phase. The relative intensity of additional new peak was weak compared to the 40 min hydrogenated sample without Na_2EDTA. Note that the conductivity of ferrites immersed in the Na_2EDTA solution without hydrogen charging was stable.

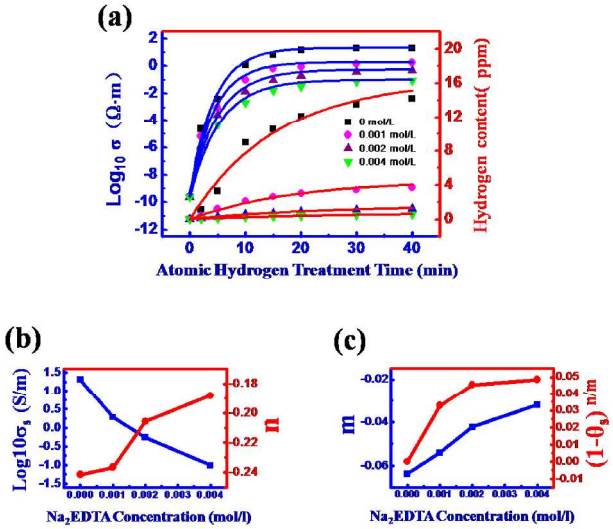

FIGURE 4. Influences of the chelating agent Na_2EDTA on the kinetics of the material modifications and hydrogen incorporation. (a)

Atomic hydrogen-induced conductivity enhancement of the ferrite and the mass content of penetrated hydrogen in electrolytes with different concentrations of Na_2EDTA. Best fits to the experimental data through Eqns. 1 and 2 using a least-squares method are given in line. The high goodness of fit *R* reveals the validity of the kinetics equations. The conductivity transformation and penetrated hydrogen amount in electrolytes without Na_2EDTA are shown for comparison. (b) and (c) plot $lg\sigma_s$ and *n*, and *m* and $(1-\theta_s)^{(n/m)}$ as a function of the Na_2EDTA concentration, respectively.

Through best fits to the experimental data, the function between the conductivity and charging time is derived by considering the boundary condition that the virgin conductivity is σ_0 (Eqn. 1).

$$lg\sigma = a \cdot e^{nt} + b \quad (1)$$

where $a = lg\frac{\sigma_0}{\sigma_s}$ and $b = lg\sigma_s$, σ, σ_0 and σ_s are the conductivity at the hydrogen charging time *t*, the virgin conductivity and the steady conductivity when the conductivity tends to remain constant, respectively. *n* is an exponential parameter obtained through best fit.

The penetrated hydrogen amount as a function of time is expressed by Eqn. 2 well.

$$q = k \cdot e^{mt} + l \quad (2)$$

Where *q* is the amount of penetrated hydrogen in the ferrite, and *k*, *l* and *m* are parameters obtained through best fit. Furthermore, the quantitative relationship between the conductivity and penetrated hydrogen amount $\sigma = f(q)$ can be derived.

Following our observations, the kinetics of the conductivity transformation and hydrogen incorporation can be discussed quantitatively with further reference to adsorption theory. Suppose that the adsorption and desorption take place on a dense solid surface, which is the case for the present study. The pseudo-first-order Lagergren kinetics model considers that the adsorption rate is proportional with the number of unoccupied active sites.[27] Through integration of adsorption rate and considering the boundary condition that $\theta=0$ at $t=0$, we have the integral as

$$\theta = \theta_s(1 - exp(-A_a \cdot C \cdot e^{-\frac{E_a}{RT}} \cdot t)) \quad (3)$$

Where θ and θ_s are the surface coverage of hydrogen atoms at the time *t* and saturation coverage, respectively. *C* is the concentration of hydrogen atoms in the electrolyte near the solid surface, E_a is the activation. energy for adsorption, *R* is the molar gas constant, *T* is the Kelvin temperature, A_a is a rate constant for the adsorption. The atomic hydrogen concentration *C* is dependent on the liquid flow rate and the cathodic reaction kinetics. A_a depends on the temperature and characteristics of the solid surface and hydrogen atoms.

Note that the hydrogen penetration is kinetically synchronous with the hydrogen adsorption. Therefore, we have $m = -A_a \cdot C \cdot e^{-E_a/RT}$. Given that the terms of *C* and $e^{-E_a/RT}$ remain unchanged, A_a is proportional with *m*. Furthermore, the function between the atomic hydrogen coverage and the conductivity can be derived by combining Eqns. 1 and 3, as given in Eqn. 4.

$$lg\sigma = a \cdot (1 - \theta/\theta_s)^{n/m} + b \quad (4)$$

From best fits to the experimental data using Eqns. 1 and 2, $lg\sigma_s$, *n* and *m* vs. Na_2EDTA concentration are derived (Fig. 4 (b) and (c)). It can be seen that $lg\sigma_s$ decreases with Na_2EDTA concentration, which corresponds to the conductivity transformation extent. The parameters of n and m change upon addition of Na_2EDTA, reflecting the competitive adsorption between Na_2EDTA and hydrogen.

The alterations in the conductivity enhancement upon addition of Na_2EDTA in the electrolytes can be a result of the exchange adsorption between Na_2EDTA and atomic hydrogen. With increasing Na_2EDTA concentration, its competitive adsorption became stronger and the atomic hydrogen coverage decreased, leading to a decrease in $lg\sigma_s$ and delaying the conductivity enhancement. More importantly, this helps to identify the rate-limiting step of the conductivity transformation in the ferrite as the atomic hydrogen adsorption; while the dissolution occurs rather fast. Here, it is pointed out that the hydrogen incorporation kinetics would probably differ from materials to materials. The rate-limiting step may be either of the adsorption or dissolution, or both for other oxides.

By substituting *b* values into Eqn. 1, the saturation coverage θ_s of atomic hydrogen as a function of Na_2EDTA concentration is obtained, as plotted in the form of $(1-\theta_s)^{n/m}$ in Fig. 4(c). The obtained adsorption isotherm has a similar shape with those reported typically for Na_2EDTA chemisorption actually.[35,36] This reflects that the characteristics of the oxide surface are altered remarkably by adsorption of Na_2EDTA.

In order to better understand the kinetics correlation among the hydrogen adsorption, hydrogen incorporation and conductivity enhancement, we altered the temperature of Na_2SO_4 solution. With increasing temperature, the enhancements of the conductivity and hydrogen content are accelerated (Fig. 5). The conductivity and the hydrogen content meet the exponential relationship of Eqn. 1 and Eqn. 2 respectively. According to Arrenius Equation the activation energy E_a for the chemisorption of atomic hydrogen is calculated to be 8.23 kJ/mol which is higher than the Van der Waals' force (about 4 kJ/mol).

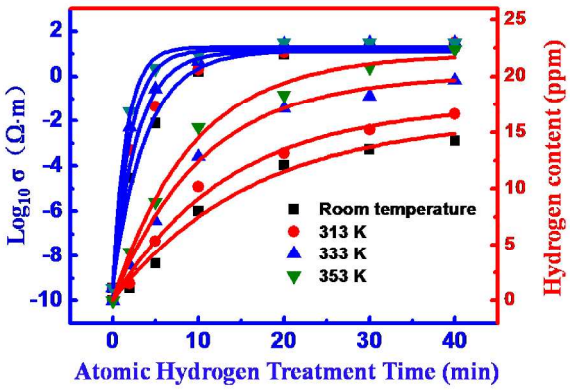

FIGURE 5. The conductivity and hydrogen content enhancements of hydrogenated ferrites charged under different temperatures.

4. Conclusions

Here, we report that a giant conductivity enhancement in $ZnFe_2O_4$ ferrite can be obtained by atomic H-charging. This work has also demonstrated unambiguously a new approach to tuning the conductivity transformation and hydrogen incorporation effectively using the chelating agent Na_2EDTA as additive. The kinetics of atomic hydrogen penetration is crucial for gaining a full understanding of hydrogen-induced modifications in a wide range of oxide materials. Quantitative kinetics correlations among the hydrogen incorporation, hydrogen adsorption and the modifications were established. Our findings clarified the role of chemisorption of atomic

hydrogen in the conductivity transformation of ferrites. The present study offers implications on controlling and utilization of atomic hydrogen-induced modifications in oxide materials. The kinetics of hydrogen-induced modifications could be adjusted by manipulating the kinetic factors of the hydrogen incorporation. Furthermore, the induced metallic state in $ZnFe_2O_4$ is fairly stable in air and water, together in consideration of the quick and cost effective transformation under moderate conditions, broadening the scope for future technical applications and research.

Acknowledgements

Authors thank the support of Program for Fundamental Research Funds for the Central Universities (FRF-SD-12-027A), New Century Excellent Talents in Universities (NCET-12-0778), Special Project on Innovative Method from the Ministry of Science and Technology of China (2012IM030500).

Notes and references

[a]Institute of Advanced Materials and Technology, University of Science and Technology Beijing, 100083 Beijing, China
[b]Department of Applied Physics, Hong Kong Polytechnic University, Hong Kong, China
[c]Department of Chemistry, Tsinghua University, Beijing 100084, China
[d]Tsinghua-Tongfang Functional Ceramics Joint Laboratory, Tongfang Co., Ltd, Beijing 100083, China.
*Author to whom correspondence should be addressed; Electronic mail: perov@sina.com

Electronic Supplementary Information (ESI) available: Detailed schematic of the set-up for atomic hydrogen charging, XRD patterns. See DOI: 10.1039/b000000x/

1 C. G. Van de Walle, Phys. Rev. Lett., 2000, **85**, 1012-1015.
2 H. Y. Huang, W. Y. Chu, Y. J. Su, J. X. Li, L. J. Qiao and S. Q. Shi, Appl. Phys. Lett., 2006, **89**, 142904.
3 N. Baluc, K. Abe, J. L. Boutard, V. M. Chernov, E. Diegele, S. Jitsukawa, A. Kimura, R. L. Klueh, A. Kohyama, R. J. Kurtz, R. Lasser, H. Matsui, A. Moslang, T. Muroga, G. R. Odette, M. Q. Tran, B. Van der Schaaf, Y. Wu, J. Yu and S. J. Zinkle, Nucl. Fusion, 2007, **47**, 696-717.
4 Q. Li, J. Liu, W. L. Lv, L. B. Mo, D. W. Duan, H. W. Gu, F. Z. Ding, T. Tang, D. L. Luo and J. L. Cao, Int. J. Hydrogen Energ., 2013, **38**, 4266-4271.
5 Y. Liu, Y. B. Guan, Y. X. Zhang, G. R. Rossman, J. M. Eiler and L. A. Taylor, Nat. Geosci., 2012, **5**, 779-782.
6 A. Fujishima and K. Honda, Nature, 1972, **238**, 37-38.
7 X. Chen, L. Liu, P. Y. Yu and S. S. Mao, Science, 2011, **331**, 746.
8 M. Ni, M. K. H. Leung, D. Y. C. Leung and K. Sumathy, Renew. Sust. Energ. Rev., 2007, **11**, 401-425.
9 A. R. Berzins and P. A. Sermon, Nature, 1983, **303**, 506.
10 R. Haugsrud and T. Norby, Nat. Mater., 2006, **5**, 193-196.
11 K. Takeuchi, C. K. Loong, Jr. J. W. Richardson, J. Guan, S. E. Dorris and U. Balachandran, Solid State Ionics, 2000, **138**, 63-77.
12 C. G. Van de Walle and J. Neugebauer, Nature, 2003, **423**, 626-628.
13 T. Li, H. M. Fan, J. B. Yi, T. S. Herng, Y. W. Ma, X. L. Huang, J. M. Xue and J. Ding, J. Mater. Chem., 2010, **20**, 5756-5762.
14 M. Vasilopoulou, A. Soultati, D. G. Georgiadou, T. Stergiopoulos, L. C. Palilis, S. Kennou, N. A. Stathopoulos, D. Davazoglou and P. Argitis, J. Mater. Chem. A, 2014, **2**, 1738-1749.
15 J. L. Cao, L. T. Li and Z. L. Gui, J. Mater. Chem., 2001, **4**, 1198-1200.
16 M. Wu, H. Y. Huang, W. Y. Chu, L. Q. Guo, L. J. Qiao, J. Y. Xu and T. Y. Zhang, J. Phys. Chem. C, 2010, **114**, 9955-9960.
17 H. Y. Huang, W. Y. Chu, Y. J. Su, K. W. Gao, J. X. Li and L. J. Qiao, J. Am. Ceram. Soc., 2007, **90**, 2062-2066.
18 V. K. Sharma and G. D. Varma, J. Appl. Phys., 2007, **102**, 056105.
19 W. P.Chen, Y.Wang, J. Y.Dai, S. G.Lu, X. X.Wang, P. F.Lee, H. L. W.Chan and C. L.Choy, Appl. Phys. Lett.,2004, **84**, 103-105.
20 W. P. Chen, Y. Wang and H. L. W. Chan, Appl. Phys. Lett., 2008, **92**, 112907.
21 Y. Wang, B. Meyer, X. Yin, M. Kunat, D. Langenberg, F. Traeger, A. Birkner and Ch. Woll, Phys. Rev. Lett., 2005, **95**, 266104.
22 W. P. Chen, Y. Wang, K. Zhu, Y. M. Hu, J. L. Cao and H. L. W. Chan, Jpn. J. Appl. Phys., 2010, **49**, 051103.
23 J. L. Cao, X. H. Wang, L. Zhang and L. T. Li, Mater. Lett., 2002, **2**, 386-391.
24 J. L. Cao, L. T. Li and L. Zhang, J. Electrochem. Soc., 2002, **149**, 89-92.
25 W. P. Chen, H. L. W. Chan, F. C. H. Yiu, K. M. W. Ng and P. C. K. Liu, Appl. Phys. Lett., 2002, **80**, 3587-3589.
26 K. J. McDonald and K. S. Choi, Chem. Mater., 2011, **23**, 4863-4869.
27 G. B. Sun, B. X. Dong, M. H. Cao, B. Q. Wei and C. W. Hu, Chem. Mater., 2011, **23**, 1587-1593.
28 W. J. Wang, S. P. Gumfekar, Q. J. Jiao and B. X. Zhao, J. Mater. Chem. C, 2013, **1**, 2851-2859.
29 J. F. Moulder, W. F. Stickle, P. E. Sobol and K. D. Bomben, Handbook of X-Ray Photoelectron Spectroscopy, Perkin Elmer Corporation, U.S.A., October, **1992**.
30 J. V. Badding, R. J. Hemley, and H. K. Mao, Science, 1991, **253**, 421-424.
31 W. Plieth, Electrochemistry for Materials Science, Elsevier Inc. **2008**.
32 H. J. Butt, K. Graf and M. Kappl, Physics and Chemistry of Interfaces, Wiley-VCH, **2006**.
33 E. M. Pierce, D. W. Wellman, A. M. Lodge and E. A. Rodriguez, Environ. Chem., 2007, **4**, 260-270.
34 F. Roncaroli and M. A. Blesa, Phys. Chem. Chem. Phys., 2010, **12**, 9938-9944.
35 P. X. Wu, J. B. Zhou, X. P. Wang, Y. P. Dai, Z. Dang, N. W. Zhu and J. H. Wu, Desalination, 2011, **277**, 288-295.
36 M. Calderón, C. Moraga, J. Leal, L. Agouborde, R. Navia and G. Vidal, Bioresource Technol., 2008, **99**, 8130-8136.